Local Flow and Concentration Evolution in Pre-mixed and In-situ Mixing Multicomponent Droplets

Xin Ye[1], Yinchuang Yang[1], Dong Liao[1], Huihe Qiu[1,2]
[1]Department of Mechanical and Aerospace Engineering,
The Hong Kong University of Science and Technology,
Clear Water Bay, Kowloon, Hong Kong SAR, China
xyeah@connect.ust.hk; yyangbv@connect.ust.hk; dliaoab@connect.ust.hk; meqiu@ust.hk

[2]Sustainable Energy and Environment Thrust,
The Hong Kong University of Science and Technology (Guangzhou),
Nansha, Guangzhou, China 511453
meqiu@ust.hk

Abstract - We investigated the local concentration evolution in pre-mixed and in-situ mixing ethanol/water multicomponent sessile droplets during the evaporation process on a hydrophobic substrate. Local concentration tracking experiments were conducted through a technique based on the aggregate-induced emission (AIE) effect, to investigate the characteristics of the concentration distribution and their formation mechanism. A consistent pattern of concentration distribution was observed in a pre-mixed multicomponent droplet: A high water fraction was detected in a shell-shaped region near the liquid-air interface, and a secondary concentration gradient existed within this shell-shaped region. After the preliminary mixed state, where the low-density ethanol predominantly accumulated at the upper position and the high-density water at the lower position, the evolution of concentration distribution can be divided into three distinct stages according to their different distribution patterns. In the early stage, a low-high-low ethanol concentration distribution appeared along the liquid-air interface from the apex region to the triple line region. In the intermediate stage, a region with high ethanol fraction was formed near the triple line, while the central region showed a high water fraction. Finally, a stable non-uniform concentration distribution emerged in the late evaporation stage, which was similar to that observed in a pre-mixed droplet. Additionally, a sudden increase of local water fraction took place at the triple line in this late evaporation stage, resulting in a change of surface tension and the subsequent depinning of the triple line.

Keywords: multicomponent evaporation, local concentration distribution, multicomponent droplet, AIE

1. Introduction

The evaporation of a multicomponent droplet on a substrate is a complicated phenomenon that plays a critical role in a wide range of scientific and industrial applications, including inkjet printing [1], micro- and nano-fluidics [2], DNA self-assembly [3], thermal management [4], combustion engineering [5], etc., and has been extensively studied in recent decades. Therefore, understanding the evaporation mechanisms of multicomponent droplets is critical for relevant technological applications. Sefiane et al. [6] observed the evaporation of ethanol/water multicomponent droplets and discovered three evaporation stages: a first stage in which the preferential evaporation of the more volatile component is dominant, a second transitional stage with an increase in contact angle and a decrease in the droplet diameter, and a third stage mainly associated with the evaporation of the less volatile component. He et al. [7] used particle image velocimetry (PIV) technique to investigate the internal flow behaviors in an evaporating multicomponent droplet, and defined the three evaporation stages based on internal flow patterns.

The concentration distribution significantly affects its evaporative behaviors during the evaporation process of the multicomponent droplet. Therefore, understanding the concentration distribution and the mechanisms underlying its evolution is crucial for the control and optimization of the evaporation of the multicomponent droplet. Studies focused on the concentration distribution evolution have motivated researchers to develop various methods for measuring the concentration of the multicomponent droplet during its evaporation. These methods include inferring concentration profiles

from infrared (IR) images [8], obtaining composition information through cavity enhanced Raman scattering (CERS) and laser-induced fluorescence [9], applying an acoustic high-frequency echography technique to track concentration changes [10], and directly quantifying the concentration using gas chromatography (GC) [11]. Although these studies successfully revealed the average concentration of the multicomponent droplet, further investigation is still required to explore the local concentration gradient inside the droplet and its effects on evaporative behaviors.

The recent development of aggregation-induced emission (AIE) luminogens has provided a novel technique for local concentration measurement [12]. When AIE luminogens are dissolved in a high-solubility solvent, they are nearly non-emissive. However, with the adding of a poor solvent, AIE huminogens show a significant increase in fluorescence emission because of the formation and accumulation of aggregates, which is known as AIE effect. Using AIE luminogens as probes, local concentration within the multicomponent droplet can be tracked, and thus the concentration evolution of multicomponent droplets can be characterized according to the change in the fluorescence emission intensity.

In this study, real-time local concentration distribution inside the ethanol/water multicomponent droplet was measured using AIE-based techniques. The evolution of local concentration distribution in both pre-mixed droplets and in-situ mixing droplets were probed and visualized.

2. Materials Preparation and Experimental Setup

The AIE luminogens utilized in this study is AIE^{TM} pH (AIEgen Biotech Co., Limited). These AIE luminogens display high solubility in ethanol but limited solubility in water, leading to a rough increase in fluorescence intensity with increasing water fraction due to the AIE effect. Thus, these concentration-sensitive AIE luminogens were used to track the local concentration evolution during the evaporation process of ethanol/water multicomponent droplets. A saturated solution of these AIE luminogens was prepared by adding ethanol to powdered AIE luminogens until complete dissolution. Then, 0.5 mL saturated AIE luminogen solution and 1 mL ethanol were thoroughly mixed to obtain da ilute AIE luminogen solution. Subsequently, 5 µL dilute solution was transferred to an EP tube, and appropriate amounts of ethanol and deionized water were added to obtain 50 µL multicomponent solution with varying waterfractionsn ranging from 50% vol. to 90% vol. All solutions were immediately used right after it is ready. The aggregates of AIE luminogens exhibit high thermal stability up to 298 °C, which is well above the maximum substrate temperature in this study (~48 °C), ensuring their stability throughout the entire experimental process.

We fabricated a 2 cm × 2 cm hydrophobic substrate for evaporation experiments. A 100 nm-thick ITO layer was coated onto a transparent glass substrate, serving as a resistive heater to heat the droplet. Two 300 nm-thick gold electrodes were fabricated on the ITO surface as electrodes. The fabrication process involved several steps. First, a photoresist pattern was created on the substrate using photolithography method for electrode patterning. Next, a 10-nm thick titanium layer was deposited on the substrate as an adhesion layer between the ITO layer and the gold layer. Subsequently, a 300-nm thick gold layer was sputtered onto the substrate, covering the titanium layer. The substrate was then immersed into acetone to remove the unwanted titanium and gold areas with photoresist, forming electrode patterns. The deposition of both metal layers was produced using ARC-12M sputtering system in NFF (HKUST). Finally, the substrate with gold electrodes was immersed in a solution of n-hexane with 0.5% vol. 1H, 1H, 2H, 2H-Perfluorodecyltriethoxysilane (FAS) for 1 hour, followed by a heating procedure in an oven of 180 °C for 1 hour to achieve hydrophobicity. The treated substrate exhibited a static contact angle of 106° (± 2°) for pure water.

The experimental setup is illustrated in Fig. 1. A pre-mixed multicomponent droplet with a volume of 6 µL was generated using a 10 µL syringe (700 Series Hand-fitted Syringe, Hamilton), and gently placed on the hydrophobic substrate. Besides, the evaporation of an in-situ mixing droplet was also investigated. For in-situ mixing, a 5-µL pure water droplet was initially generated by the 10-µL syringe and placed on the substrate, followed by the generation of a pendant 5-µL ethanol droplet from the same syringe. The ethanol droplet was then gently brought into contact with the water droplet on the apex and mixed. Both droplets were seeded with AIE luminogens.
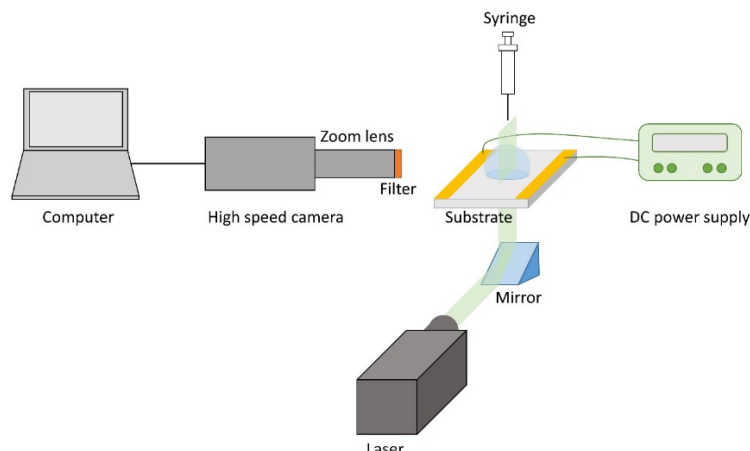
Fig. 1: Schematic of the experimental setup.

The hydrophobic substrate was bonded to a customized printed circuit board (PCB) via the gold electrodes, and was heated to 48 °C using a DC power supply. A continuous laser system served as the excitation source for AIE luminogens. The laser emitted light at a wavelength of 450 nm, which was expanded to form a light sheet and aligned to illuminate the central profile of the seeded droplet. High-speed imaging was conducted using a high speed CCD camera (FASTCAM SA-Z, Photron) with a zoom lens (MP-E 65mm f/2.8 1-5x Macro Photo, Canon) at a resolution of 1024 × 1024 pixels during droplet evaporation process. To eliminate the interference of extraneous light sources, including the incident laser, a 550-nm long-pass filter is positioned in front of the lens, permitting only the fluorescence emission to pass through and enter the CCD camera. The droplet profile image sequences were recorded at a frame rate of 500 fps and a shutter time of 1/1000 s.

3. Results and Discussion
3.1. AIE-based Local Concentration Tracking in A Pre-Mixed Droplet
Given the high laser power employed in this study, the influence of photobleaching on fluorescence intensity is significant so that cannot be ignored. Photobleaching is a photo-chemical reaction that irreversibly damages the fluorophore molecules upon excitation [13]. Consequently, fluorophore molecules lose their capability on fluorescence emission, leading to a decrease in the total fluorescence intensity over time. Necessary corrections were applied to the real-time fluorescence intensity based on the photobleaching curve, as depicted in Fig. 2. The photobleaching curve was fitted using a negative bi-exponential model, as proposed in previous research [13]. The corrections made to the fluorescence intensity take into account the effect of photobleaching, and ensure that the data obtained from the experiments are relatively accurate.

In Fig. 3, the fluorescence intensity in multicomponent solutions with different water fractions was measured and presented. Three measurements were taken at every water fraction. The fluorescence intensity demonstrates a gradual increase as the water fraction increases progressively. It is noteworthy that the fluorescence intensity exhibits a significant increase within the water fraction range from 65% vol. to 75% vol. At a water fraction of 85% vol., the fluorescence intensity is approximately 12 times higher than that of the solution with a water fraction of 50% vol. However, an abnormal decline in fluorescence intensity was observed when the water fraction reached 90% vol., which can be ascribed to the self-absorption effect resulting from the accumulation of large luminogen aggregates in massive poor solvent water. Linear fitting was conducted within the water fraction range from 55% vol. to 85% vol. to calibrate the local concentration. By establishing a correlation between the fluorescence intensity and water fraction, the local concentration of multicomponent droplets in subsequent experiments can be calculated.
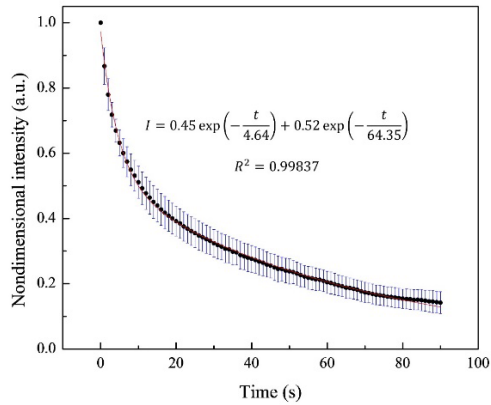
$$I = 0.45 \exp\left(-\frac{t}{4.64}\right) + 0.52 \exp\left(-\frac{t}{64.35}\right)$$

$$R^2 = 0.99837$$

Fig. 2: Photobleaching curve as time elapsed.

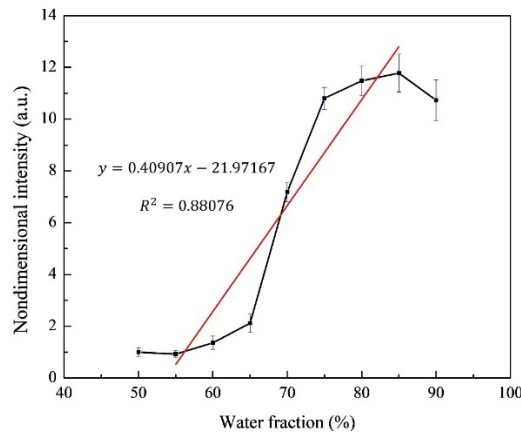$$y = 0.40907x - 21.97167$$

$$R^2 = 0.88076$$

Fig. 3: Plot of nondimensional fluorescence intensity versus water fraction in ethanol/water multicomponent solution.

Fig. 4 demonstrates the snapshots of the evaporation process of a multicomponent droplet at room temperature of 21 °C and a heated substrate of 48 °C, respectively. Droplets in both cases have an initial composition of 40% vol. ethanol and 60% vol. water. In addition, Fig. 4 illustrates the derived real-time concentration profiles, reflecting the evolution of the local concentration distribution. The mean water fraction in the droplet increases progressively due to the preferential evaporation of ethanol, leading to the gradual strengthening of fluorescence intensity over time. On the spatial dimension, the fluorescence intensity was observed to be higher in the proximity of the liquid-air interface, which is a shell-shaped region, as compared to the inner region. This is because ethanol evaporates from the liquid-air interface, resulting in the high water fraction near the surface. Moreover, a secondary concentration gradient merges within the shell-shaped region. The concentration profiles indicate that the water fraction is highest at the apex region of the droplet, and gradually decreases along the liquid-air interface, reaching the lowest value at the triple line region. This phenomenon can be attributed to the internal Marangoni flow at the droplet bottom, which facilitates the radical transportation of ethanol from the interior of the droplet to the triple line region, thereby maintaining a relatively low water fraction near the triple line region. Hence, a concentration gradient is formed along the droplet surface, extending from the triple line to the apex.
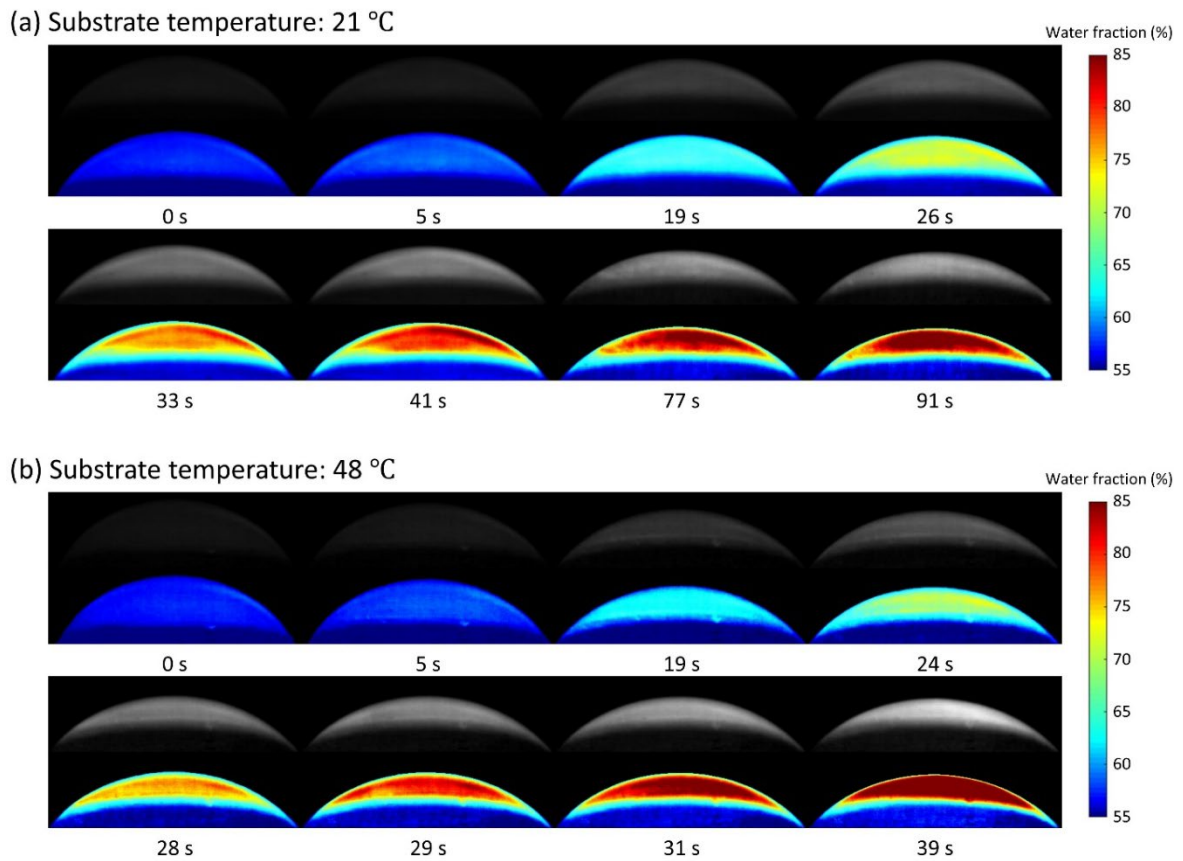
Fig. 4: Snapshots and concentration profiles of evaporating pre-mixed multicomponent droplets with an initial concentration of 40% ethanol + 60% water at substrate temperature (a) 21 °C and (b) 48 °C.

Notably, a sudden increase of fluorescent intensity at the triple line occurs at the late period of evaporation as shown in Fig. 5. The phenomenon is always followed by the depinning of the triple line. This can be explained as follow: as the total content of ethanol decreases, the decreasing surface tension gradient could not support a strong Marangoni flow continually, thus the ethanol replenishment toward the triple line region is insufficient. Hence, the water fraction at the triple line increases abnormally, leading to a sudden increase in fluorescence intensity. Besides, because of the shortage of ethanol replenishment at the triple line region, the local surface tension increases, driving the depinning and retraction of the triple line.
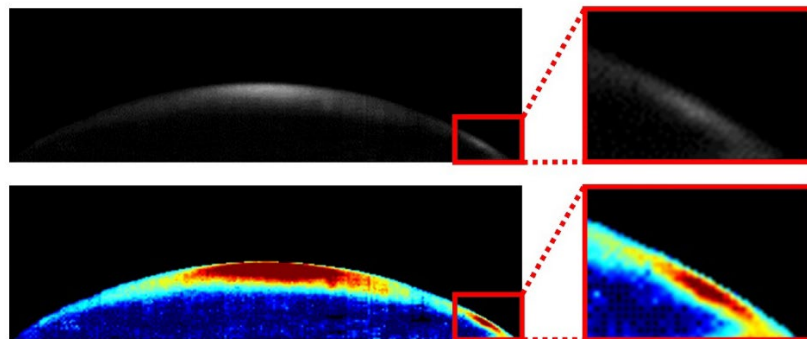

Fig. 5: Snapshots of the sudden increase of fluorescent intensity.

3.2. AIE-based Local Concentration Tracking in An In-situ Mixing Droplets

Fig. 6 shows the evolution of local concentration inside the in-situ mixing multicomponent droplet during the mixing and subsequent evaporation processes. All images were photobleaching corrected. Since ethanol is a good solvent of AIE luminogens, the pure ethanol droplet with AIE luminogens has almost no fluorescence emission. When the ethanol droplet contacts the water droplet, a relatively strong fluorescence emission occurrs at the contact interface of the two droplets. The phenomenon can be explained as follow: a multicomponent layer is formed in situ due to the diffusion of two components at the interface, driving the formation of aggregates of AIE luminogens, thus the fluorescence intensity increases. Ethanol and water are then mixed under the effects of diffusion and internal flow. The diffusion time scale can be calculated by Eq. 1:

$$\tau_d = r^2/D \tag{1}$$

where r is the droplet radius and D is the diffusion coefficient. After calculation, the diffusion time scale of ethanol in a 10 µL droplet is ~39 min, which is much longer than the mixing time (in the scale of seconds). Therefore, it can be concluded that the mixing process is dominated by internal flow. Chaotic and furious vortices appear at the surface due to the random distribution of ethanol and water at the beginning period of contact and mixing, contributing to the preliminary mixing of the multicomponent droplet. An in-situ mixing droplet has a different initial distribution of ethanol and water compared with a pre-mixed sessile droplet. At the preliminary mixed state, the fluorescence intensity at the upper position is slightly lower than that at the bottom position. This is because the density of ethanol is lower than that of water.
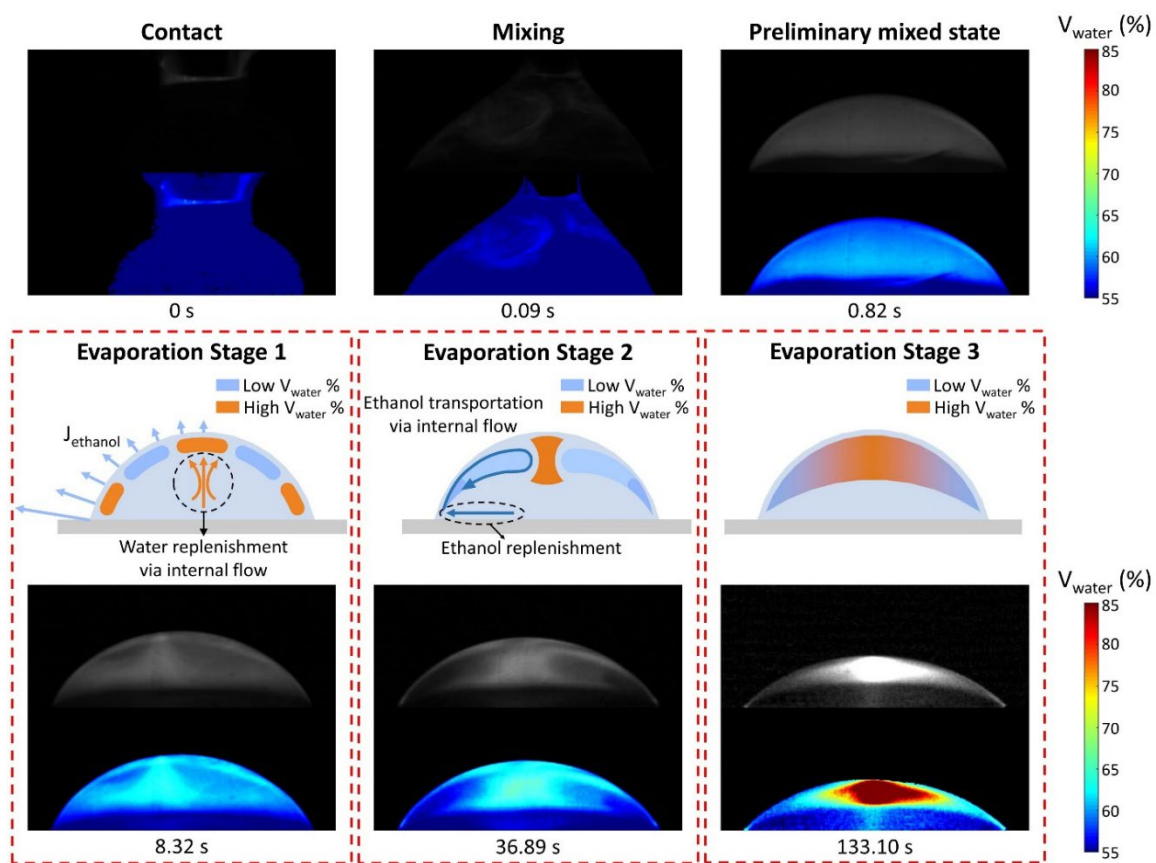

Fig. 6: Snapshots and concentration profiles of the evaporating in-situ mixing multicomponent droplet with schematics of three evaporation stages.

Evaporation significantly affects the subsequent evolution of the local concentration inside the multicomponent droplet after the short preliminary mixing process. At the early stage of evaporation, water assembles at the bottom and ethanol assembles at the upper position, and a concentration gradient occurs along the surface. Hence Marangoni flow dominates at this stage, leading to an internal flow upward at the central axis. Water at the lower position inside the droplet migrates to the apex via the internal flow, resulting in a low local ethanol concentration at the apex region. Besides, the loss of ethanol is maximum at the triple line according to the distribution of evaporative flux (J), so the local ethanol concentration at the triple line region decreases to a relatively low level. Therefore, a high ethanol concentration region appears at the shoulder position of the droplet, forming a low-high-low ethanol concentration distribution along the liquid-air interface.

An intermediate stage starts when the ethanol concentration at the shoulder position decreases to a certain level due to ethanol evaporation and ethanol transportation toward the triple line region via internal flow. At this stage, the ethanol concentration at the triple line region is relatively high due to ethanol replenishment, thus a concentration gradient is formed. A Marangoni flow with an opposite direction replaces the dominant role of the former Marangoni flow. Therefore, ethanol is gradually transported along the liquid-air interface via this Marangoni flow from the triple line to the apex region, accounting for an expansion of the low fluorescence emission region along the liquid-air interface. At the central region far away from the vortices, replenishment of ethanol depends on the slow diffusion process. Thus, the ethanol concentration maintains a low level, i.e. the water fraction is high, leading to strong fluorescence emission at the central region. Notably, the phenomenon of the early and the intermediate stages only take place in in-situ mixing droplets, since the different initial distribution of ethanol and water leads to different internal flow behaviors that contribute to the phenomenon.

After fully developing the intermediate stage, it transfers to the late stage, which exhibits a steady distribution of fluorescence emission similar to the evaporating pre-mixed sessile droplet. This distribution shows that water mainly assembles at the outer shell-shaped cap of the droplet, with a secondary concentration gradient along the liquid-air interface. This late stage will last until the droplet completely evaporates.

4. Conclusion

AIE-based local concentration tracking was conducted on a pre-mixed multicomponent droplet and an in-situ mixing multicomponent droplet, respectively.

For a pre-mixed sessile multicomponent droplet, a stable concentration distribution was revealed. A shell-shaped cap was predominantly composed of water, since ethanol evaporated preferentially at the liquid-air interface. Moreover, a secondary concentration gradient was identified within the shell-shaped cap, where the apex region exhibited the highest water fraction and the triple line region displayed the lowest. This was attributed to the ethanol replenishment toward the triple line via the Marangoni flow. At the late stage of the evaporation process, there occurred a sudden increase in ethanol concentration, followed by the depinning of the triple line. This was due to the inadequate ethanol replenishment resulting from the weakening of the Marangoni flow.

For an in-situ mixing multicomponent droplet, the evaporation process can be divided into three stages based on the concentration distribution. The early stage of evaporation following the preliminary mixed state was dominated by the solutal Marangoni flow due to the non-uniform initial distribution of two components. During the early stage of evaporation, a low-high-low ethanol concentration distribution appeared along the liquid-air interface from the apex to the triple line. The explanation indicated that water was replenished from the lower position to the apex region via the Marangoni flow, and ethanol mostly evaporated at the triple line, leading to low ethanol concentrations at the apex region and at the triple line region respectively. Subsequently, it transferred to the intermediate stage when ethanol concentration at the shoulder position decreased to a relatively low level. In the intermediate stage of evaporation, another Marangoni flow in opposite direction became dominant since the re-distribution of two components. Hence, ethanol migrated upward along the surface via the Marangoni flow, causing the high-ethanol-concentration region to expand along the droplet surface. The ethanol concentration at the apex region was low because ethanol replenishment to the apex region was by slow diffusion process

rather than by fast convective flow. After full development of the intermediate stage, the concentration distribution turned to be similar to that of a pre-mixed droplet, indicating the transition to the late stage.

Acknowledgments

References

[1] Park, J. and J. Moon, "Control of colloidal particle deposit patterns within picoliter droplets ejected by ink-jet printing", *Langmuir,* vol. 22, no. 8, pp. 3506-3513, 2006.

[2] Sbarra, S., L. Waquier, S. Suffit, A. Lemaître, and I. Favero, "Optomechanical measurement of single nanodroplet evaporation with millisecond time-resolution", *Nature Communications,* vol. 13, no. 1, pp. 6462, 2022.

[3] Agarwal, S., M.A. Klocke, P.E. Pungchai, and E. Franco, "Dynamic self-assembly of compartmentalized DNA nanotubes", *Nature Communications,* vol. 12, no. 1, pp. 3557, 2021.

[4] Hu, Y., T. Liu, X. Li, and S. Wang, "Heat transfer enhancement of micro oscillating heat pipes with self-rewetting fluid". *Int, J, Heat Mass Tran.,* vol. 70, no. pp. 496-503, 2014.

[5] Sazhin, S.S., "Modelling of fuel droplet heating and evaporation: Recent results and unsolved problems", *Fuel,* vol. 196, pp. 69-101, 2017.

[6] Sefiane, K., L. Tadrist, and M. Douglas, "Experimental study of evaporating water-ethanol mixture sessile drop: influence of concentration"l *Int. J. Heat Mass Tran.,* vol. 46, no. 23, pp. 4527-4534, 2003.

[7] He, M.H. and H.H. Qiu, "Internal flow patterns of an evaporating multicomponent droplet on a flat surface", *Int. J. Therm. Sci.,* vol. 100, pp. 10-19, 2016.

[8] Katre, P., P. Gurrala, S. Balusamy, S. Banerjee, and K.C. Sahu, "Evaporation of sessile ethanol-water droplets on a critically inclined heated surface", *Int. J. Multiphase Flow,* vol. 131, pp. 103368, 2020.

[9] Hopkins, R.J., R. Symes, R.M. Sayer, and J.P. Reid, "Determination of the size and composition of multicomponent ethanol/water droplets by cavity-enhanced Raman scattering", *Chem. Phys. Lett.*, vol. 380, no. 5, pp. 665-672, 2003.

[10] Chen, P., M. Toubal, J. Carlier, S. Harmand, B. Nongaillard, and M. Bigerelle, "Evaporation of Binary Sessile Drops: Infrared and Acoustic Methods To Track Alcohol Concentration at the Interface and on the Surface", *Langmuir*, vol. 32, no. 38, pp. 9836-9845, 2016.

[11] Li, W., R. Chen, X. Zhu, Q. Liao, D. Ye, Y. Yang, and D. Li, "Photothermally Caused Propylene Glycol–Water Binary Droplet Evaporation on a Hydrophobic Surface", *Industrial & Engineering Chemistry Research*, vol. 60, no. 10, pp. 4153-4167, 2021.

[12] Chen, S.J., J.Z. Liu, Y. Liu, H.M. Su, Y.N. Hong, C.K.W. Jim, R.T.K. Kwok, N. Zhao, W. Qin, J.W.Y. Lam, K.S. Wong, and B.Z. Tang, "An AIE-active hemicyanine fluorogen with stimuli-responsive red/blue emission: extending the pH sensing range by "switch+knob" effect", *Chem. Sci.*, vol. 3, no. 6, pp. 1804-1809, 2012.

[13] Vicente, N.B., J.D. Zamboni, J.F. Adur, E.V. Paravani, and V.H. Casco. Photobleaching correction in fluorescence microscopy images. in Journal of Physics: Conference Series, 2007, vol. 90, no. 1, pp. 012068.